Derivation of Clear-Air Turbulence Parameters from High-Resolution Radiosonde Data

E. MARTINI

Department of Information Engineering and Mathematics, University of Siena, Siena, and Wave Up S.r.l., Florence, Italy

A. FRENI

Department of Information Engineering, University of Florence, Florence, Italy

F. CUCCOLI

Radar and Surveillance System National Laboratory, National Interuniversity Consortium for Telecommunications (CNIT), Pisa, Italy

L. FACHERIS

Department of Information Engineering, University of Florence, Florence, Italy

(Manuscript received 18 February 2016, in final form 4 October 2016)

ABSTRACT

The knowledge of atmospheric refractive index structure constant (C_n^2) profiles is fundamental to determine the intensity of turbulence, and hence the impact of the scintillation impairment on the signals propagating in the troposphere. However, their relation with atmospheric variables is not straightforward, and profiles based on statistical considerations are normally employed. This can be a shortcoming when performing simulations for which scintillation disturbances need to be consistent with the assumed atmospheric conditions. To overcome this limitation, this work describes a procedure to obtain an estimate of the refractive index structure constant profile of clear-air turbulence under given atmospheric conditions. The procedure is based on the application of the vertical gradient approach to high-resolution radiosonde data. Since turbulence is known to be confined to vertically thin layers, a preliminary identification of turbulent layers is required. This is accomplished by analyzing the profiles of the Richardson number. The value of the outer scale length is estimated using the Thorpe length calculated from the potential temperature profile. The procedure is applied to high-resolution radiosonde data that have been acquired from the Stratosphere–Troposphere Processes and their Role in Climate (SPARC) Data Center, and the obtained results are consistent with measured C_n^2 profiles previously published in the literature.

1. Introduction

Scintillation consists of rapid fluctuations of phase and amplitude of a radiowave propagating though the troposphere, and it can significantly alter the propagation of microwave signals (Wheelon 2001, 2003). It is caused by dynamical turbulence, related to wind velocity fluctuations, which induces small-scale atmospheric inhomogeneity by turbulent mixing; these, in turn, are related to turbulent refractive index fluctuations, which are responsible for tropospheric scintillation. The impact of scintillation disturbance is particularly significant when considering methods for sounding the atmosphere by means of radio waves that propagate from a transmitter to a receiver in a limb geometry. In such a context, correctly modeling the scintillation effects is of paramount importance to evaluate the performance and the potential of the sounding approach. Martini et al. (2006) have developed a theoretical model for analyzing the scintillation effects due to turbulence on a radio link between two low-Earth-orbiting (LEO) satellites. This model has been used to investigate the potential of an approach referred to as normalized differential spectral attenuation (NDSA), whose objective is to estimate the total content of water vapor (WV)

Corresponding author e-mail: Luca Facheris, luca.facheris@unifi.it

DOI: 10.1175/JTECH-D-16-0046.1

along the radio link connecting two LEO satellites (Facheris et al. 2008). However, the turbulence parameters in that model were not related to the ''local'' conditions of the atmosphere: more precisely, the fact that the profiles of the refractive index structure constant C_n^2 (which is directly related to the intensity of scintillation) could not be coherently associated with such conditions was a deficiency of the model.

This paper presents a novel procedure capable of providing the C_n^2 profile at microwave frequencies corresponding to a given atmospheric situation under clear-air conditions, in the altitude range of 0–20 km. The proposed procedure is based on the computation of the vertical gradient of the potential refractive index from high-resolution radiosonde observations (raobs). A similar approach has been first outlined by Van Zandt et al. (1978) and successively refined as shown in Van Zandt et al. (1981). However, in these works the computation of the layers' thickness and the estimate of intermittency effects are not rigorously based, and this constitutes an intrinsic problem for applying such an approach. Van Zandt et al. (1978) assumed a constant thickness of the turbulent layers throughout the troposphere and considered its value as a free variable to be set so as to obtain the best overall fit with structure constant profiles obtained from Doppler radar measurements. Successively, Van Zandt et al. (1981) determined the turbulent fraction of the atmosphere based on only statistical considerations, since the coarseness of the available atmospheric profiles did not allow them to identify the fine structure of the atmospheric variables. Later on, similar methods have been applied to a large set of radiosonde data to obtain statistical distributions of turbulence parameters as made, for instance, by D'Auria et al. (1993), Vasseur and Vanhoenacker (1998), and Vasseur (1999). In particular, Vasseur and Vanhoenacker (1998) identified the turbulent layers from the abrupt changes in the C_n^2 profiles. Later on, Vasseur (1999) considered the outer scale as a random variable with a prescribed probability density function and used a probabilistic approach to estimate the mean value of the structure constant parameter.

In this paper, the procedure for the derivation of the structure constant profiles is made self-consistent by combining the vertical gradient approach with an estimate of the turbulence layered structure for each single radiosonde ascent. This is done by using high-resolution raobs to capture the fine structure of the atmospheric variables, which allows, on the one hand, to exploit the analysis of the Richardson number to identify the turbulent layers and, on the other hand, to employ the Thorpe length estimated from temperature data to derive the vertical profile of the outer scale length. Numerical results obtained by applying the proposed procedure to radiosonde data taken from the Stratospheric–Troposphere Processes and their Role in Climate (SPARC) Data Center/U.S. high-resolution radiosonde data (available online at atmos.sparc.sunysb.edu, directory: /pub/sparc/hres) are consistent with measured or calculated profiles presented in the literature.

The paper is organized as follows: in section 2 we introduce the refractive index structure constant, while in section 3 we discuss the possible approaches to estimate its vertical profiles in the troposphere, and we identify the most effective one for our purposes. In section 4 we discuss the possible meteorological data sources and introduce the one used in this work. The proposed procedure is described step by step in section 5. Then, in section 6, we present and discuss the numerical results. The sensitivity to atmospheric data errors is investigated in section 7. Finally, conclusions are drawn in section 8.

2. Characterization of atmospheric turbulence

The refractive index n of a turbulent atmosphere can be decomposed into its average value and a small component that is a stochastic function of position and time:

$$n(\mathbf{r},t) = \langle n(\mathbf{r},t)\rangle + \delta n(\mathbf{r},t), \tag{1}$$

where the angle brackets $\langle\cdot\rangle$ indicate the ensemble average. The fluctuating component δn, which gives rise to electromagnetic scintillation, can be described as a zero-mean locally stationary process (Ishimaru 1999). In the microwave and millimeter wave frequency band, the refractive index is given by

$$n = 1 + \frac{77.6}{T}\left(p + 4810\frac{e}{T}\right)10^{-6}, \tag{2}$$

where T is the temperature (K), p is the atmospheric pressure (mbar) and e is the partial pressure of the measured water vapor (mbar) (Smith and Weindtraub 1953). The fluctuations of the refractive index are therefore related to the fluctuations of T, p, and e as follows:

$$\delta n \times 10^6 = \delta T\left[-\frac{77.6}{T^2}\left(p + 9620\frac{e}{T}\right)\right] + \delta p\frac{77.6}{T} + \delta e\frac{373\,256}{T^2}. \tag{3}$$

Therefore, the refractive index fluctuations depend on both temperature and humidity fluctuations, while pressure variations provide a negligible contribution.

The refractive index structure function $D_n(\boldsymbol{\rho})$ is defined as the mean-square value of the difference

between the fluctuating components at two different positions:

$$D_n(\boldsymbol{\rho}) = \langle [\delta n(\mathbf{r}, t) - \delta n(\mathbf{r} + \boldsymbol{\rho}, t)]^2 \rangle. \quad (4)$$

According to the Kolmogorov theory (Kolmogorov 1962), for separation distances $|\boldsymbol{\rho}|$ such that $l_0 < |\boldsymbol{\rho}| < L_0$, where l_0 and L_0 are the inner and outer scale of turbulence, respectively, the structure function obeys a universal law, independent of the large-scale boundary conditions and the mechanism of energy dissipation. This theory has been verified by numerous experiments using both fluids and gases (Arneodo et al. 1996). In this range, called inertial range, the refractive index structure function is well approximated by the following law:

$$D_n(\boldsymbol{\rho}) = C_n^2 |\boldsymbol{\rho}|^{2/3}, \quad (5)$$

where C_n^2 is the refractive index structure constant. Hence, this constant represents the amplitude of the spatial correlation of the refractive index fluctuations between two points at unitary distance.

The refractive index structure constant provides a measure of the intensity of the refractive index fluctuations. For this reason, it is a quantity of paramount importance—along with the outer scale length—for the estimate of turbulence effects on radio signals that propagate in the lower atmosphere. For instance, an estimate of the height profile of C_n^2 in the troposphere is needed to assess the impact of scintillation on the microwave link between two LEO satellites. Once this profile is known, prediction models based on theoretical studies (see, for instance, Tatarskii 1961; Wheelon 2001, 2003; Ishimaru 1999) can be used to relate this quantity to the corresponding scintillation effects (Martini et al. 2006). Karasawa et al. (1988) and Otung (1996) developed empirical formulations to describe the structure constant behavior. However, they are based on specific measured data and cannot be easily generalized. On the contrary, in this work we want to derive C_n^2 from a specific distribution of atmospheric parameters, so that scintillation estimates can be tailored to any given atmospheric condition.

Measurements of C_n^2 profiles have revealed a significant dependency on altitude (C_n^2 decreases by some orders of magnitude from the lower to the higher troposphere) and significant variation (even one order of magnitude) from one day to the following one. There is also experimental evidence that turbulence in the free atmosphere is confined to thin horizontal layers separated by nonturbulent regions. These layers are limited in horizontal extent and time. The gross turbulence in these layers is therefore inherently inhomogeneous, anisotropic, and nonsteady. Nevertheless, in the interior of a turbulent layer, the turbulence may be expected to be nearly homogeneous and isotropic and (considering an observation interval significantly shorter than the turbulence decorrelation time) close to a steady state (Van Zandt et al. 1978).

3. Methods for deriving the turbulence parameters from meteorological data

Several methods have been developed to derive the refractive index structure constant profiles. Some of them rely on direct measurements made with instrumented balloons carrying pairs of refractometers (Crain 1950). Others are based on the analysis of turbulence effects on the propagation of the microwave signals [e.g., measurements with pulse Doppler radars, as shown in Gossard et al. (1982)], while the rest rely on the measurement or simulation of atmospheric parameters (temperature, humidity, wind velocity) combined with a proper turbulence model. The methods belonging to the first two groups require ad hoc propagation experiments. Hence, they could not be applied for the objective of this work. For this purpose, the methods of the third group are the most appropriate ones and have therefore been considered. These approaches are critically reviewed in the following section.

a. Methods for deriving the structure constant profiles

Three approaches can be considered to derive the C_n^2 profiles from standard meteorological data: the first one relies on the Hufnagel formula (Hufnagel 1978), the second one is based on the computation of the structure constants of temperature and humidity (Wesely 1976; Burk 1980), and the third one relates the value of C_n^2 to the vertical gradient of the potential refractive index and to the outer scale of turbulence (Tatarskii 1961). The first approach cannot be used for our purposes, since it does not account for the humidity contribution; therefore, at microwave and millimeter frequencies, it is valid only in the upper portion of the troposphere. The second approach can be applied only to the lowest part of the troposphere, since it relies on assumptions that are verified only in the boundary layer. The third approach is more general and can be used in the microwave and millimeter wave ranges throughout the troposphere, but it also requires the knowledge of the vertical outer scale and of turbulence layering.

In the following sections, the structure function and the vertical gradient approaches are discussed in more detail.

1) STRUCTURE FUNCTION APPROACH

The contributions of temperature and moisture fluctuations to C_n^2 may be expressed in terms of both their

individual and mutual structure parameters (Wyngaard et al. 1978):

$$C_n^2 = B_1 C_T^2 + B_2 C_{eT} + B_3 C_e^2, \tag{6}$$

where C_T^2 and C_e^2 are the temperature and humidity structure constants, respectively, and C_{eT} is the joint structure parameter of temperature and humidity. Expressions for the constants appearing in Eq. (6) are provided by Wesely (1976). The structure constants C_T^2, C_{eT}, and C_e^2 can be deduced from measured atmospheric quantities. This approach is based on the assumption that temperature and humidity structure functions follow simple scaling laws, which is valid in the boundary layer (Burk 1980; Hill et al. 1988; Andreas 1988). In particular, the validity of the Monin–Obukhov similarity is usually assumed in this context (Monin and Obukhov 1954). However, since its validity is not proven above the boundary layer, the application of this approach to the derivation of the refractive index structure constant is normally restricted to the lower troposphere.

2) Vertical gradient approach

The vertical gradient approach for the derivation of the refractive index structure constant relies on Tatarskii's model of the microstructure of the refractive index in a turbulent flow, according to which atmospheric turbulence is related to the vertical gradient of the wind velocity (Tatarskii 1961). Tatarskii has demonstrated that, for any concentration of a conservative passive additive ϑ with mean value $\overline{\vartheta}$, the structure constant can be written as

$$C_\vartheta^2 = a^2 L_v^{4/3} \left(\frac{\partial \overline{\vartheta}}{\partial z}\right)^2, \tag{7}$$

where a is a constant and L_v is the vertical outer scale of turbulence. Conservative passive additives are quantities that have no effect on the statistical analysis of the turbulence dynamics; however, they are transported and mixed by the wind velocity fluctuations. Equation (7) can be used to estimate C_n^2 after expressing the refractive index in terms of conservative passive additives (Tatarskii 1961). Absolute temperature and humidity are not conservative in this meaning, since a parcel of air changes its temperature and humidity when moved up or down in the atmosphere. To properly apply Eq. (7), Eq. (2) is rewritten in terms of conservative quantities. In the absence of condensation, these quantities can be the potential temperature and the specific humidity, respectively.

The potential temperature θ of a parcel of fluid at pressure p is defined as the temperature that the parcel would acquire if adiabatically brought to the standard pressure of 1000 mbar:

$$\theta = T\left(\frac{1000}{p}\right)^{R/c_p}, \tag{8}$$

where T is the current absolute temperature (K) of the parcel, R is the universal gas constant (J kg^{-1} K^{-1}), and c_p is the specific heat (J kg^{-1} K^{-1}) at constant pressure. For air $R/c_p = 0.286$.

The water vapor pressure can be expressed in terms of the specific humidity q, which represents the concentration of water vapor in the air (i.e., the ratio of the mass of water vapor in air to the total mass of the mixture of air and water vapor) and is given by

$$q = \frac{0.622e}{p - 0.378e}. \tag{9}$$

By inserting Eqs. (8) and (9) into Eq. (2), one gets

$$n = 1 + \frac{77.6}{\theta} p \left(\frac{1000}{p}\right)^{R/c_p} \left[1 + 7800 \frac{q}{\theta}\left(\frac{1000}{p}\right)^{R/c_p}\right] 10^{-6}. \tag{10}$$

When air parcels are displaced in the atmosphere by turbulent mixing, inhomogeneities are created because the characteristics of the displaced air parcels differ from the characteristics of the environment. The pressure of the displaced parcels undergoes a continuous equalization with the environmental pressure. This process changes the temperature and water vapor pressure of the air parcels. Their potential temperature and specific humidity, however, are preserved provided that no condensation occurs. This implies that, if a parcel of air from level z_1 appears at level z_2 as a result of the action of turbulent mixing, the quantities θ and q do not change, while the pressure p takes the new value $p(z_2)$. As a consequence, the value of the refractive index will differ from the local one by the quantity

$$\delta n = n[\theta(z_1), q(z_1), p(z_2)] - n[\theta(z_2), q(z_2), p(z_2)]. \tag{11}$$

Therefore, only conservative quantities can be considered when computing the mean vertical gradient M that has to be inserted into Eq. (7),

$$M = \frac{\partial n}{\partial \theta}\frac{\partial \theta}{\partial z} + \frac{\partial n}{\partial q}\frac{\partial q}{\partial z}, \tag{12}$$

which is also called the vertical gradient of the "potential" refractive index (Ottersten 1969). One finally obtains (Van Zandt et al. 1978)

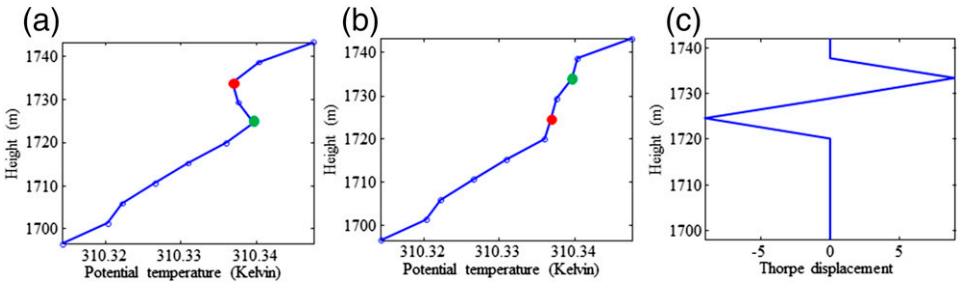

FIG. 1. The procedure for the determination of the Thorpe length. (a) Actual potential temperature profile. (b) Rearranged monotonic potential temperature profile. (c) Thorpe displacement.

$$M = -\frac{77.6p}{T}\times 10^{-6}\frac{\partial \ln\theta}{\partial z}\left[1 + 15\,600\frac{q}{T}\left(1 - \frac{1}{2}\frac{\dfrac{\partial \ln q}{\partial z}}{\dfrac{\partial \ln\theta}{\partial z}}\right)\right], \tag{13}$$

where $g/c_p = 9.8\times 10^{-3}\,\mathrm{km}^{-1}$. It is noted that the contribution of specific humidity to M is normally negligible above 10–12 km. In that range of altitude, Eq. (13) could therefore be simplified by retaining only the first term inside the square brackets.

In accordance with Eq. (7), the refractive index structure constant of a turbulent region can be estimated from M as

$$C_n^2 = 2.8L_v^{4/3}M^2. \tag{14}$$

3) CHOICE OF THE APPROACH

The approach based on the use of the structure function concept makes some particular assumptions on the turbulence structure, and it is suitable for analyzing turbulence only in the lower troposphere. Conversely, the approach based on the vertical gradient of the refractive index can be applied throughout the whole troposphere; consequently, we have chosen this second approach in order to obtain a procedure that is applicable to all the altitudes of our interest. However, two additional steps are required: the computation of L_v and the identification of the turbulent layers. These steps are discussed in the following sections.

b. Estimate of the vertical outer scale length

The vertical outer scale length L_v is thought to be of the order of the thickness of the turbulent layers, and values ranging from a few meters above the Earth surface to several hundreds of meters in the free atmosphere are found in the literature (see, for instance, Crain 1955; Nath et al. 2010; Ziad et al. 2004). This large variability is however plausible, as it is known that the outer scale of turbulence depends significantly on meteorological conditions and therefore may vary over some orders of magnitude with altitude, time, and location.

Van Zandt et al. (1978) derived the vertical outer scale by using Eq. (14) and by selecting L_v so that the theoretical C_n^2 matches the values derived from radar measurements: following this approach, Van Zandt found that an appropriate value is 10 m. D'Auria et al. (1993) calculated the mean value of the refractive index structure constant by assuming the vertical outer scale length is randomly variable with a prescribed probability density function. An alternative approach for the estimate of L_v that does not rely on statistical considerations is based on the determination of the Thorpe length L_T from potential temperature profiles. Thorpe's length is an empirical estimate of the length scale of turbulent overturning in a stratified turbulent medium. It was first applied by Thorpe to the analysis of turbulence in lake water (Thorpe 1977), but it can be also applied to turbulence in the free atmosphere (Clayson and Kantha 2008) by using the fact that potential temperature is a conservative property of the fluid particles, like the density in water.

It is based on the assumption that inversions are the result of turbulent stirring, since a stable atmosphere would be characterized by a monotonic potential temperature profile. The method consists of rearranging an observed potential temperature profile that may contain inversions into a stable monotonic profile that contains no inversions. If the sample at depth z_n must be moved to depth z_m to generate the stable profile, the Thorpe displacement is $|z_m\text{-}z_n|$. The method is illustrated in Fig. 1. The Thorpe length is defined as the root-mean-square of the Thorpe displacement and is proportional to the Ozmidov length L_O, $L_O \cong 0.9L_T$, which, in turn, is proportional to L_v according to the relation $L_v \cong L_O/2.27$ (Clayson and Kantha 2008). Since the Thorpe length is directly related to local atmospheric parameters, we have chosen this approach to estimate the vertical outer scale length.

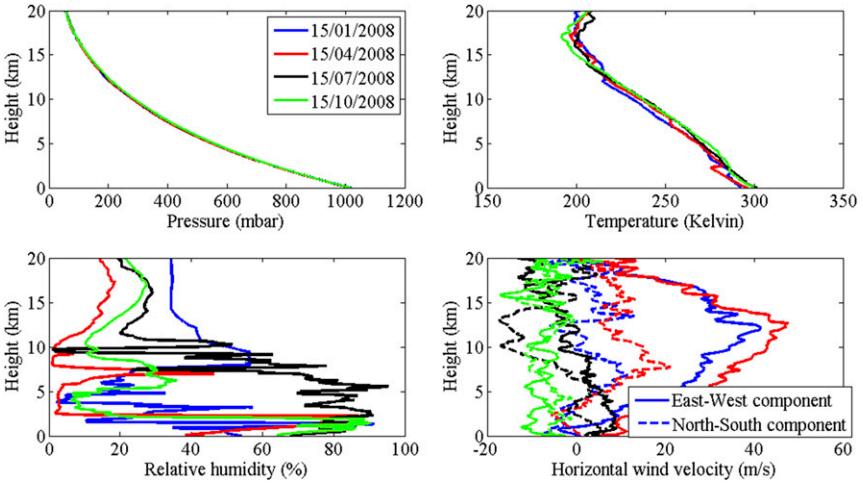

FIG. 2. Pressure, temperature, relative humidity, and wind velocity profiles from GPS radiosonde launched at Miami at 0000 UTC 15 Jan, 15 Apr, 15 Jul, and 15 Oct 2008.

c. *Intermittency*

In the free atmosphere, turbulence is confined to layers with a large horizontal extent but quite thin along the vertical direction, with sharp randomly variable boundaries and limited temporal extent, separated by nonturbulent regions (see Barat and Bertin 1984; Rees 1991). This means that the clear air may be locally fluctuating between unstable and stable conditions, and that turbulence may be intermittent (D'Auria et al. 1993). Intermittency effects are due to the variability of atmospheric parameters that are supposed to have large-scale fluctuations in addition to small-scale fluctuations.

The average value of C_n^2 can be soundly calculated through Eq. (14) only in the turbulent layers; contributions from layers without turbulence should instead be ignored. For this reason, in many cases the mean value of C_n^2 estimated by using measured meteorological quantity and Eq. (14) appears higher than that obtained from radars or microwave satellite links (D'Auria et al. 1993). Van Zandt et al. (1978) assumed that the atmosphere is turbulent in regions where the wind shear exceeds a critical value and that the statistical distribution of the wind shears is described by the simple model introduced by Rosenberg and Dewan (1975).

In this work, we want to identify the turbulent layer starting from the analysis of the meteorological data, without making any a priori assumption. Indeed, if the resolution with which atmospheric variables are known

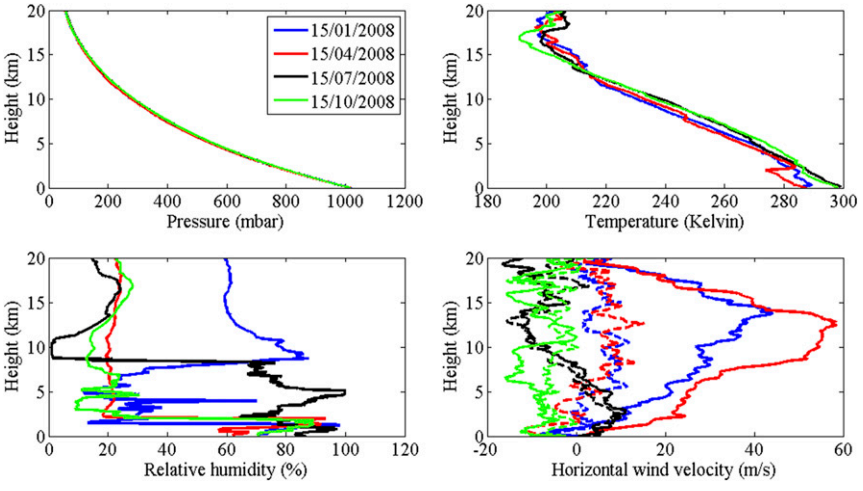

FIG. 3. Pressure, temperature, relative humidity and wind velocity profiles from GPS radiosonde launched at Miami at 1200 UTC 15 Jan, 15 Apr, 15 Jul, and 15 Oct 2008.

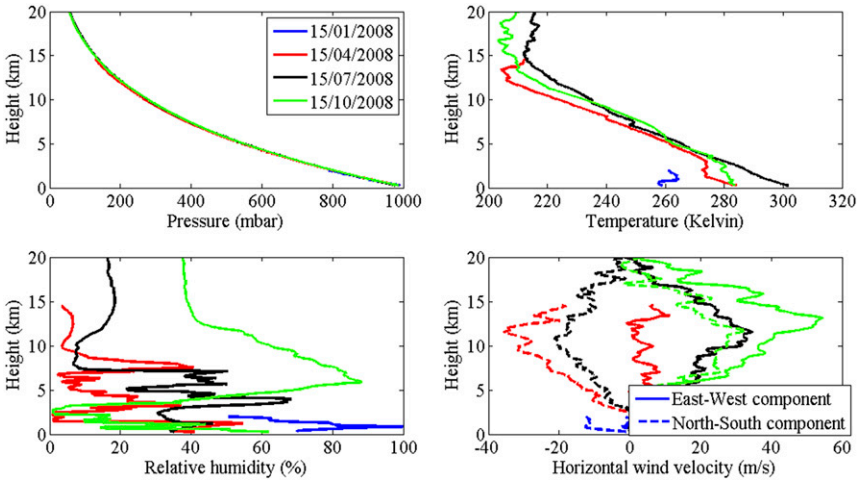

FIG. 4. Pressure, temperature, relative humidity, and wind velocity profiles from GPS radiosonde launched at Minneapolis at 0000 UTC 15 Jan, 15 Apr, 15 Jul, and 15 Oct 2008.

is comparable with the layer thickness, one can set a local condition in order to identify the points that belong to regions with turbulence. A parameter that can be exploited to this end and that depends only on the atmospheric variables (as opposed to the Reynolds number, whose calculation requires the knowledge of the initial scale of the flow) is the Richardson number, which is the ratio between the work done against gravity and the kinetic energy: the smaller its value, the lower the stability of the flow and the higher the likelihood of turbulence. The Richardson number is defined as (Ishimaru 1999)

$$R_i = \frac{N^2}{S^2}, \tag{15}$$

where S^2 is the square wind shear, that is, the squared magnitude of the vertical gradient of the horizontal velocity (u and v being the horizontal and vertical components of the wind velocity),

$$S^2 = \left(\frac{\partial u}{\partial z}\right)^2 + \left(\frac{\partial v}{\partial z}\right)^2, \tag{16}$$

and N is the buoyancy frequency, which is also known as Brunt–Väisälä frequency (s^{-1}), namely, the frequency with which a parcel or particle of fluid displaced a small vertical distance from its equilibrium position in a stable environment would oscillate. Buoyancy frequency N is defined as

$$N = \sqrt{\frac{g}{\theta_v}\frac{\partial \theta_v}{\partial z}}, \tag{17}$$

where θ_v as in (17) is the virtual potential temperature, which for typical atmospheric conditions can be assumed equal to the potential temperature.

For $R_i = 0.25$, the available kinetic energy due to the velocity difference across the layer is equal to the work that must be done against buoyancy forces in order to exchange fluid parcels across the layer. Therefore, it is normally assumed that the condition $R_i < 0.25$ defines an unstable stratification and a developed turbulence (see Taylor 1931; Turner 1973). This information has been used by D'Auria et al. (1993) and Vasseur (1999) to calculate the mean value of C_n^2 through a probabilistic approach. In this work, it is used to identify the turbulent layers associated with a single atmospheric profile.

4. Meteorological data sources

Meteorological data can be obtained from either numerical models or direct measurements. In the following sections, we briefly discuss the advantages and disadvantages of the different data sources with respect to our purposes.

a. Numerical methods

The advantage of the numerical models is that they do not require expensive measurements with ad hoc instruments, they can be used for any site, and they have predictive capability. Two examples of numerical schemes are the large-eddy simulation (LES) (Moeng 1984) and the numerical weather prediction (NWP) models (Stephens 1984). The first approach is based on the assumption that larger scales contain most of the energy and turbulent fluxes and are more dependent on the flow environment, while the less energetic

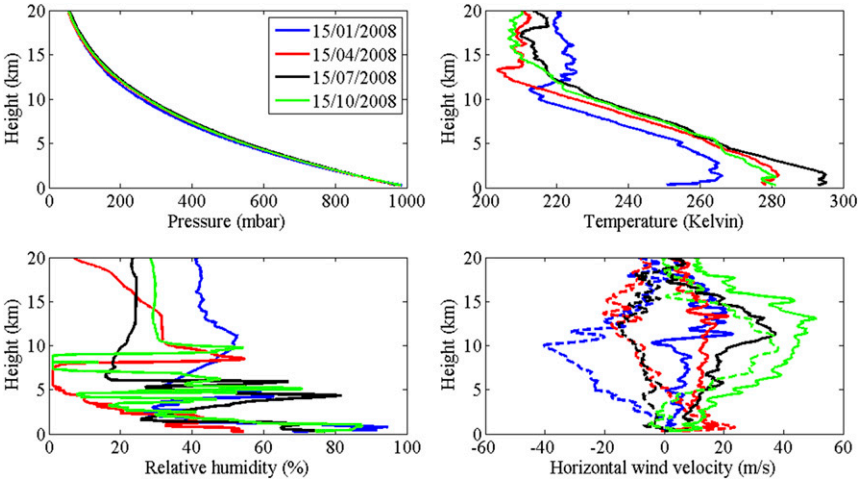

FIG. 5. Pressure, temperature, relative humidity, and wind velocity profiles from GPS radiosonde launched at Minneapolis at 1200 UTC 15 Jan, 15 Apr, 15 Jul, and 15 Oct 2008.

subgrid-scale motions are more universal in character. LES is successful for the analysis of turbulence in the planetary boundary layer, and in particular the convective boundary layer (see Moeng 1984; Deardorff 1974; Mason 1989; Siebesma and Holtslag 1996; Peltier and Wyngaard 1995; Cheinet and Siebesma 2009). The application of LES to higher altitudes, however, appears more cumbersome for various reasons. The main one is that outside the boundary layer, it is no more true that large structures are responsible for most of the vertical transport processes, which is the assumption at the basis of this approach. For this reason, LES can be quite sensitive to the type of model adopted to describe the turbulent diffusivities by subgrid-scale motions. Furthermore, in the presence of significant stable stratifications, the length scale of the vertical motions may become comparable with the minimum resolvable scale. Finally, proper boundary conditions are needed to terminate the analysis domain: in the boundary layer one can resort to the Monin–Obukhov similarity to set the boundary condition at the lower boundary, but the condition to be imposed at higher altitudes is more difficult to define. Furthermore, because of the necessity for making some assumptions about the weather conditions, LES could be useful for making some simulations and analysis but not for a statistical analysis over a year.

NWP models take as input a numerical terrain model with high spatial resolution and fields of temperature, pressure, humidity, and wind velocity at the initial time t_0 (from either measurements or forecasts), and they

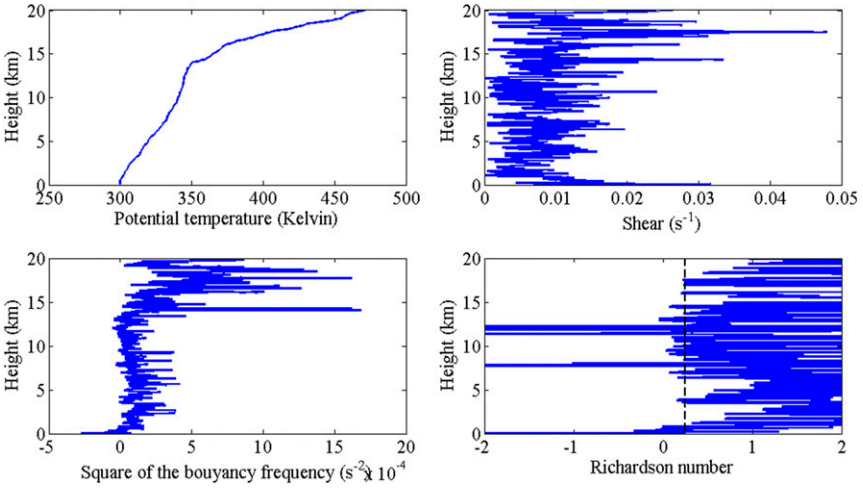

FIG. 6. Potential temperature, wind shear, buoyancy frequency, and Richardson number profiles derived from a single radiosonde launch (Miami, 0000 UTC 15 Jul 2008).

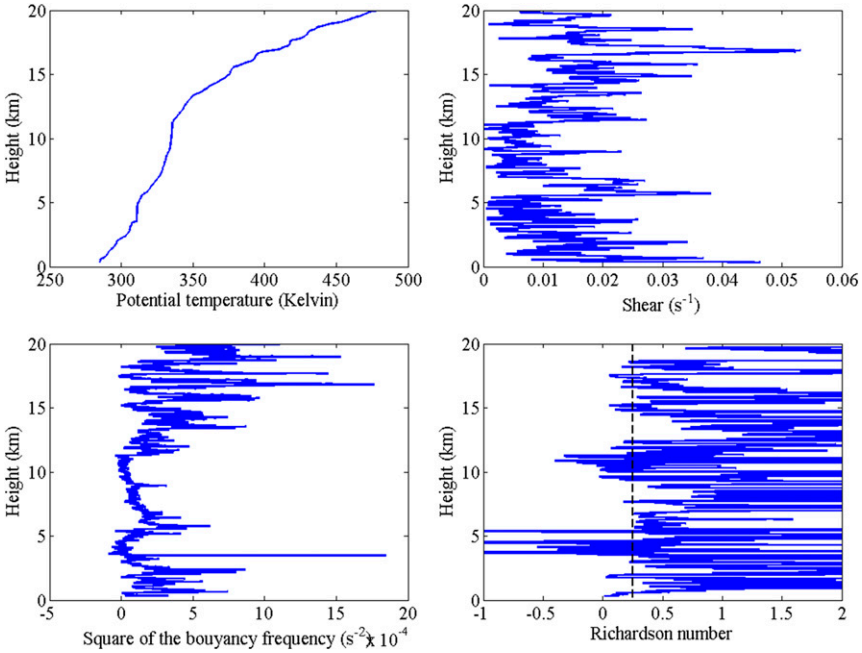

FIG. 7. Potential temperature, wind shear, buoyancy frequency, and Richardson number profiles derived from a single radiosonde launch (Minneapolis, 0000 UTC 15 Jan 2008).

simulate the evolution of atmospheric 3D motions. They can therefore provide 3D maps of meteorological parameters, and with the inclusion of a turbulence production technique, also of C_n^2. Since most NWP models cover a fairly large area, the grid spacing of even high-resolution models is necessarily coarse relative to the scale of turbulence. As a consequence, only an average C_n^2 estimate over the model grid scale can be calculated. Furthermore, most NWP models suffer from inherent smoothing and filtering effects, so that the smallest scales produced by the model are in fact underresolved. In the approaches proposed in the literature, the vertical resolution varies from tens of meters at levels nearest to the ground to hundreds of meters at the highest levels (see Masciadri et al. 1999a,b; Cherubini et al. 2008).

b. *Radiosonde data*

A radiosonde contains instruments capable of making direct in situ measurements of air temperature,

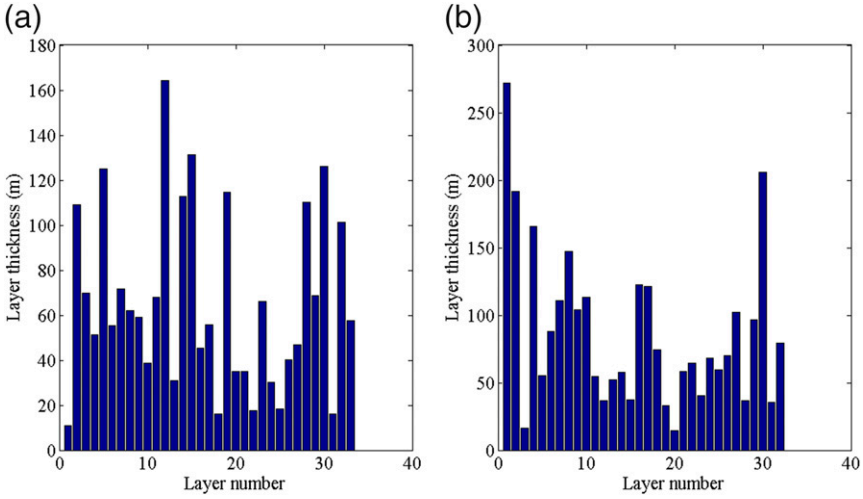

FIG. 8. Distribution of turbulent layer thicknesses as derived from the analysis of the Richardson number: (a) Miami, 0000 UTC 15 Jul 2008; and (b) Minneapolis, 0000 UTC 15 Oct 2008.

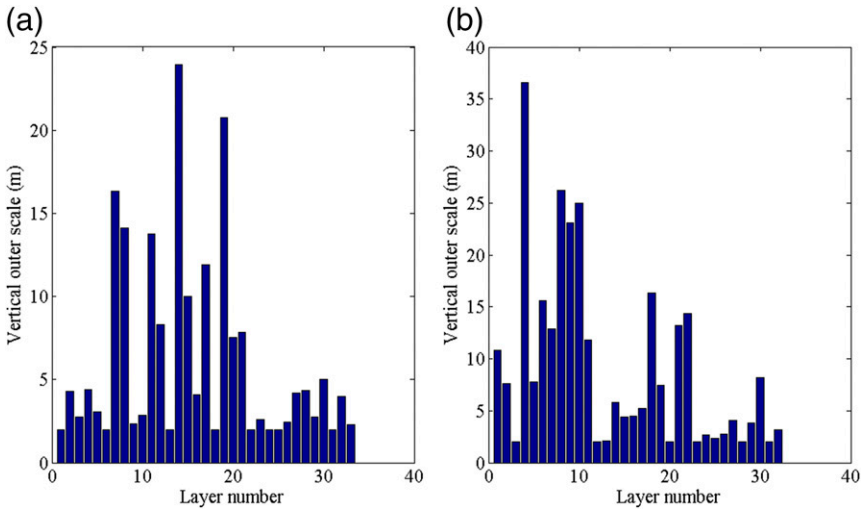

FIG. 9. Vertical outer scale estimated from the analysis of the Thorpe displacement: (a) Miami, 0000 UTC 15 Jul 2008; and (b) Minneapolis, 0000 UTC 15 Oct 2008.

relative humidity, and pressure with height, typically to altitudes of approximately 30 km. The ascent of a radiosonde also provides an indirect measure of the wind speed and direction at various levels throughout the troposphere (Brettle and Galvin 2003; Galvin 2003). There are a large number of radiosonde launch sites worldwide, even if only at some of them (mostly located in the United States and the United Kingdom) high-resolution measurements are available. The advantage of these data is that they are easily available and cover a wide range of climates over long periods of time. A drawback is that radiosonde data may contain a significant amount of noise, which is enhanced by the derivation in Eq. (13). Preprocessing of data may be required to circumvent this problem (Vanhoenacker-Janvier et al. 2009).

c. *Choice of the data source*

As discussed in the previous sections, simulated data provided by LES or NWP models are not utilizable for our purposes due to their intrinsic limitations: LES is not expected to provide a reliable description of turbulence outside the boundary layer, while NWP models have poor vertical resolution. Instead, radiosonde data can provide usable measured profiles of the atmospheric variables if the resolution is sufficiently high to resolve the turbulence fine structure (Nath et al. 2010). Since the thickness of the turbulent layers can be as small as a few meters, temporal resolutions of 1 and

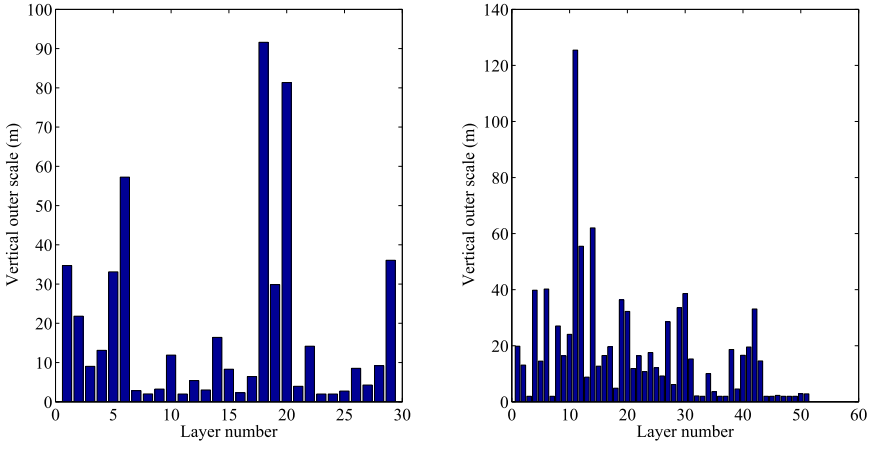

FIG. 10. Vertical outer scale estimated from the analysis of the Thorpe displacement for the radiosonde launched at (left) Lincoln, Illinois, and (right) Jacksonville, Florida, at 0000 UTC 15 Jul 2008.

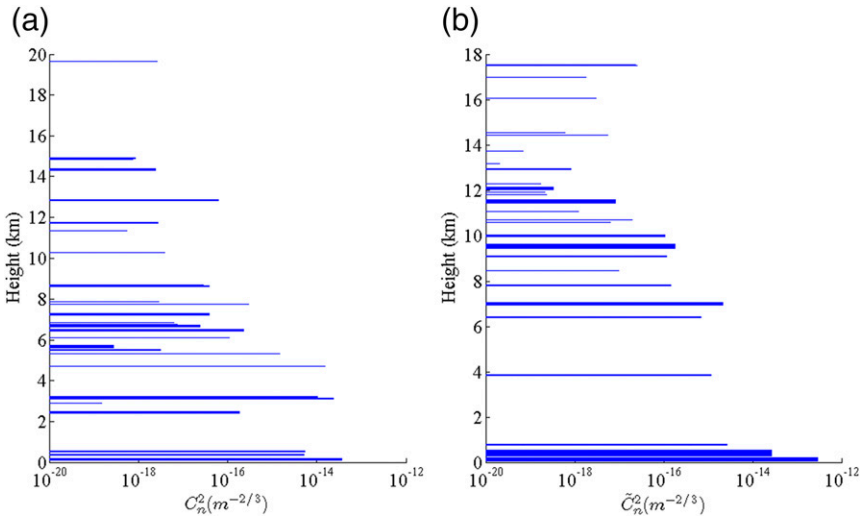

FIG. 11. Turbulence intensity profiles derived from a single radiosonde launch at Miami: (a) 0000 UTC 15 Jan 2008; and (b) 0000 UTC 15 Jul 2008.

2 s (corresponding to vertical resolutions of roughly 5 and 10 m, respectively) are optimal, but also lower resolutions, up to 6 s (corresponding to a vertical resolutions of roughly 30 m), can be acceptable. One limitation of radiosonde data is that each dataset gives only a single point in space and time (always at the same time of the day). Hence, radiosondes are not the ideal solution; however, they have the advantage of providing realistic data. For this reason, we have applied our proposed procedure for deriving C_n^2 profiles to the high-resolution raobs described in the following section.

RADIOSONDE DATABASE

Raobs from the following databases meet the high-resolution requirements for the application of the procedure described in this work:

- SPARC Data Center (ftp://atmos.sparc.sunysb.edu/pub/sparc/hres; since 2005)
- British Atmospheric Data Centre (BADC; http://badc.nerc.ac.uk; 2-s resolution since 1990)
- Atmospheric Radiation Measurement (ARM) data archive (http://www.archive.arm.gov; 2-s resolution since 1 July 2001)

All these sites also provide preprocessed data that are obtained by applying normalization, correction, outlier removal, and data plausibility checks to the raw data [see, for instance, the National Climatic Data Center data documentation for dataset 6213 (DSI-6213; Ebisuzaki 2004)]. This preprocessing is important to avoid errors in the derivative operations involved in the determination of the C_n^2 profiles (Vanhoenacker-Janvier et al. 2009).

The SPARC database refers to 54 measurement sites in the United States, and the raobs have a time resolution of 1 s. Therefore, our need to achieve a satisfactorily high vertical resolution is met, since 1 s approximately corresponds to 5 m. The measured variables comprise pressure, relative humidity, temperature, geopotential height, geometric height, wind speed, and wind direction.

BADC data are relevant to 12 measurement sites: 8 are in the United Kingdom and the others are in Gibraltar, St. Helena, and the Antarctic. The profiles are taken at 2-s intervals and contain, among others, pressure, temperature, relative humidity, humidity mixing ratio, altitude, wind speed, and wind direction.

The ARM database comprises data from the Balloon-Borne Sounding System (SONDE; see Holdrige et al. 2011), which provides vertical profiles of pressure, temperature, relative humidity, wind speed, and wind direction. Derived quantities include the geopotential altitude, and the u component and v component of wind velocity. The vertical sampling of the profiles is about 2 s. ARM data are relevant to three fixed measurement sites and nine mobile sites in the North Hemisphere, the South Hemisphere, and the tropics.

In total, 78 different measurement sites are available in Europe, the United States, the tropics, the Antarctic, and in further selected regions. The time resolution for these sites is 1–2 s, which means a vertical resolution of 5–10 m.

5. Procedure for deriving the C_n^2 profiles

The procedure starts from the analysis of the atmospheric profiles. As explained in the previous section, measured radiosonde data are used, from which the

following atmospheric variables are obtained for each geometric height z:

- p: pressure (mbar);
- RH: relative humidity (%);
- T: absolute temperature (K);
- u, v: horizontal and vertical components of the wind speed ($\mathrm{m\,s^{-1}}$). Proper smoothing is applied to remove the quantization error. This smoothing is required only to avoid errors in the derivative operations involved for the determination of the C_n^2 profiles, and it implies only a minimal adjustment of the atmospheric data, which does not introduce any unnatural effect in the proposed procedure.

a. Calculation of the refractive index vertical gradient

The following quantities are calculated from the atmospheric variables:

- θ = potential temperature (K)

$$\theta = T\left(\frac{1000}{p}\right)^{0.286} \tag{18}$$

- e_s = saturation vapor pressure (mb)

$$e_s = 6.112e^{17.67[(T-273.15)/(T-29.65)]} \tag{19}$$

- e = vapor pressure (mb)

$$e = e_s\frac{\mathrm{RH}}{100} \tag{20}$$

- q = specific humidity (dimensionless)

$$q = \frac{0.622e}{p - 0.378e}. \tag{21}$$

The vertical gradient of the potential refractive index is then calculated using Eq. (13), where the derivatives are approximated by finite-difference formulas.

b. Identification of the turbulent layers

The identification of the turbulent layers is based on the analysis of the Richardson number profiles. Calculating R_i requires, in turn, that the following quantities be computed:

- r = mixing ratio (dimensionless)

$$r = \frac{0.622e}{p - e} \tag{22}$$

- θ_v = virtual potential (K)

$$\theta_v = \theta(1 + 0.61r - r_L) \tag{23}$$

- N = buoyancy frequency ($\mathrm{s^{-1}}$)

$$N = \sqrt{\frac{g}{\theta_v}\frac{\partial\theta_v}{\partial z}} \tag{24}$$

- S = wind shear ($\mathrm{s^{-1}}$)

$$S = \sqrt{\left(\frac{\partial u}{\partial z}\right)^2 + \left(\frac{\partial v}{\partial z}\right)^2}. \tag{25}$$

In Eqs. (24) and (25), the derivatives are approximated by finite-difference formulas. From the quantities in Eqs. (22)–(25), one finally gets R_i by using Eq. (15). The condition $R_i > 0.25$ identifies a number L of turbulent layers of variable thickness. Inside each layer, L_T is obtained as the root-mean-square of the Thorpe displacement, and the vertical outer scale length L_v is obtained as $L_v = 0.3965L_T$.

c. Definition of the C_n^2 profiles

As a consequence of the previous steps, one can define the C_n^2 profiles as

$$C_n^2(z) = \sum_{l=1}^{L} C_{nl}^2 \mathrm{rect}\left(\frac{z - z_l}{\Delta z_l}\right), \tag{26}$$

where L is the number of turbulent layers that have been identified though the analysis of the Richardson number, z_l is the mean height of the lth layer, and Δz_l is its thickness. Term C_{nl}^2 is calculated for each layer by using in Eq. (14) the relevant vertical outer scale and the average value of M, and

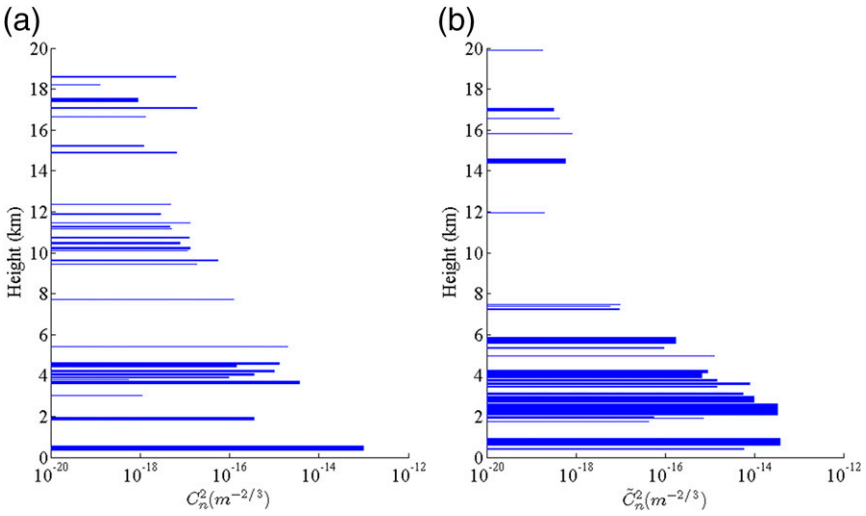

FIG. 12. Turbulence intensity profiles derived from a single radiosonde launch at Minneapolis: (a) 0000 UTC 15 Oct 2008; and (b) 1200 UTC 15 Jul 2008.

$$\text{rect}(x) = \begin{cases} 1 & \text{for} \quad |x| < \dfrac{1}{2} \\ 0 & \text{otherwise} \end{cases}. \tag{27}$$

Notice that the minimum layer thickness detectable with the proposed procedure is determined by the vertical resolution of the radiosonde data.

6. Numerical results

Sample numerical results obtained after having processed SPARC radiosonde data are shown in the following sections. In particular, the results refer to two stations: latitude: 25.74°, longitude: −80.38° (Miami, Florida) and latitude: 44.83°, longitude: −93.33° (Minneapolis, Minnesota). Selected data are from 15 January, 15 April, 15 July, and 15 October 2008, corresponding to four different seasons. Data were gathered for two time layers, 0000 and 1200 UTC. Measured variables of interest for the derivation of the C_n^2 profiles are pressure, absolute temperature, relative humidity, geometric height, and horizontal components of the wind speed. Sample profiles of the atmospheric variable relevant to the abovementioned launch sites are reported in Figs. 2–5.

a. Identification of the turbulent layers

Starting from radiosonde profiles of pressure, temperature, relative humidity, and wind velocity, all the other parameters of interest are derived following the procedure illustrated in section 5. Typical profiles of potential temperature, wind shear, buoyancy frequency, and Richardson number are reported in Figs. 6 and 7.

In the last plot, relevant to the Richardson number profiles, a vertical dashed line has been drawn at $R_i = 0.25$ in order to better identify the turbulent layers. As can be seen, there are a number of thin sporadic turbulent layers (characterized by $R_i < 0.25$) separated by larger stable regions (characterized by $R_i > 0.25$). This has been found to be a general feature of the radiosonde profiles analyzed. The distribution of the turbulent layer thicknesses for the two profiles of Figs. 6 and 7 is shown in Fig. 8, where the horizontal scale reports the layer number (starting from the lowest altitude) and the vertical scale reports the relevant thickness. As can be seen, the analysis of the Richardson number reveals that turbulence exists in thin layers that may be only a few meters thick. In this example, the vertical resolution of the radiosonde data (and, hence, the minimum detectable layer thickness) is approximately equal to 5 m, a value sufficiently small to provide information also on thin turbulent layers. The obtained layer thickness distribution, which agrees with measurements reported in the literature (see, for instance, Lüdi and Magun 2002), suggests that the turbulent outer scales in these layers cannot be larger than this, at least in the vertical direction. Furthermore, it is seen that, as a general rule, the thickest turbulent layers are located at lower altitudes.

b. Outer scale length

The vertical outer scale length of each layer is obtained by processing the radiosonde data in order to determine the value of the Thorpe length through the procedure outlined in section 3. Sample results are shown in Figs. 9 and 10, where the horizontal scale

TABLE 1. Percent error in C_n^2 profiles [defined as in Eq. (29)] corresponding to different values of injected errors in the atmospheric data for the radiosonde launch at Miami at 1200 UTC 15 Jan 2008.

Percent error in C_n^2 profiles ($\varepsilon_p = 5\%$)	$\varepsilon_T = 0$ K (%)	$\varepsilon_T = 0.1$ K (%)	$\varepsilon_T = 0.3$ K (%)
$\varepsilon_{RH} = 0\%$	0.2	1.9	4.6
$\varepsilon_{RH} = 2\%$	4.5	5.3	8.3
$\varepsilon_{RH} = 5\%$	10.2	11.2	16.2

TABLE 2. Percent error in C_n^2 profiles [defined as in Eq. (29)] corresponding to different values of injected errors in the atmospheric data for the radiosonde launch at Minneapolis at 0000 UTC 15 Oct 2008.

Percent error on C_n^2 profiles ($\varepsilon_p = 5\%$)	$\varepsilon_T = 0$ K (%)	$\varepsilon_T = 0.1$ K (%)	$\varepsilon_T = 0.3$ K (%)
$\varepsilon_{RH} = 0\%$	0.1	2	4.1
$\varepsilon_{RH} = 2\%$	4.6	5.7	7.9
$\varepsilon_{RH} = 5\%$	10.2	11.5	13.8

reports the layer number (starting from the lowest altitude). Notice that in the present paper, the outer scale length is defined as the inverse of the outer scale wavenumber κ_0, $L_0 = 1/\kappa_0$, while in other publications (e.g., Wheelon 2001, 2003) it is defined as $L_0 = 2\pi/\kappa_0$, leading to apparently larger values of L_0. As expected, the estimated vertical outer scale length is smaller or at most comparable with the layer thickness derived in the previous step of the procedure. A significant difference is found between the average outer scale values for two sets of results in Figs. 9 and 10, which confirm the wide variability of this parameter. The derived values are consistent with the ones reported in the literature—see, for instance, Nightingale and Buscher (1991), Coulman et al. (1988), and Ghosh et al. (2003).

c. *Computation of the C_n^2 profiles*

The potential refractive index gradient is calculated by applying Eq. (13). As explained above, the values of C_n^2 calculated from Eq. (14) represent a measure of the strength of turbulence only within the turbulent layers. For this reason, the actual profiles of C_n^2 to be used for scintillation calculation also account for the layered structure of turbulence according to Eq. (26). Sample final profiles are reported in Figs. 11 and 12, where the vertical scale indicates the altitude and the horizontal scale indicates the intensity of C_n^2 for each turbulent layer.

As a general trend, the average value of C_n^2 exhibits an exponential decrease with altitude. Furthermore, the analysis of different datasets has revealed that—as expected—C_n^2 is higher at lower latitudes and in warmer seasons. Observed values and behavior are coherent with the results shown in the literature (see Wheelon 2001, 2003, and references therein).

7. Analysis of sensitivity to the accuracy of radiosonde data

Since the proposed procedure relies on the use of atmospheric variables profiles that could be affected by errors, it is interesting to investigate its sensitivity to measurement errors in radiosonde data.

To this end, we have deliberately added fixed errors to temperature, pressure, and humidity profiles according to the following equations:

$$\begin{aligned} \tilde{T} &= T + \varepsilon_T \\ \tilde{p} &= p(1 + \varepsilon_p) \\ \widetilde{\mathrm{RH}} &= \mathrm{RH}(1 + \varepsilon_{\mathrm{RH}}), \end{aligned} \tag{28}$$

where T, p, and RH are the absolute temperature, pressure, and relative humidity, respectively, provided by radiosondes; ε_T is the absolute error in temperature; and ε_p and $\varepsilon_{\mathrm{RH}}$ are the relative errors in pressure and relative humidity, respectively. As a general trend, it is found that structure constant profiles are more sensitive to temperature and humidity errors than to pressure errors. For this reason, the analysis has been more focused on these two variables, for which a parametric study has been conducted. The typical accuracy for corrected data of recent radiosondes, like the ones considered in the previous section, is 5% for humidity sensors (Pereira et al. 2015) and 0.1–0.3 K for temperature sensors (Luers 1997).

To quantify the impact of radiosonde data errors on the estimate of the C_n^2 profiles, the percent error has been defined as follows:

$$\varepsilon = \frac{\int |C_n^2(z) - \tilde{C}_n^2(z)|\, dz}{\int C_n^2(z)\, dz}, \tag{29}$$

where $\tilde{C}_n^2$ and C_n^2 are the structure constant profiles calculated from the data with and without errors, respectively. Notice that the structure constant profiles in Eq. (29) are defined as in Eq. (27); that is, they are equal to zero outside the turbulent layers. For $\tilde{C}_n^2$, the location and thickness of each turbulent layer are estimated starting from meteorological data affected by errors.

The sensitivity analysis has been applied to several radiosonde datasets by considering different values for the errors in temperature (0, 0.1, and 0.3 K) and relative humidity (0%, 2%, and 5%). On top of this, a fixed error of 5% in pressure was considered in all the cases.

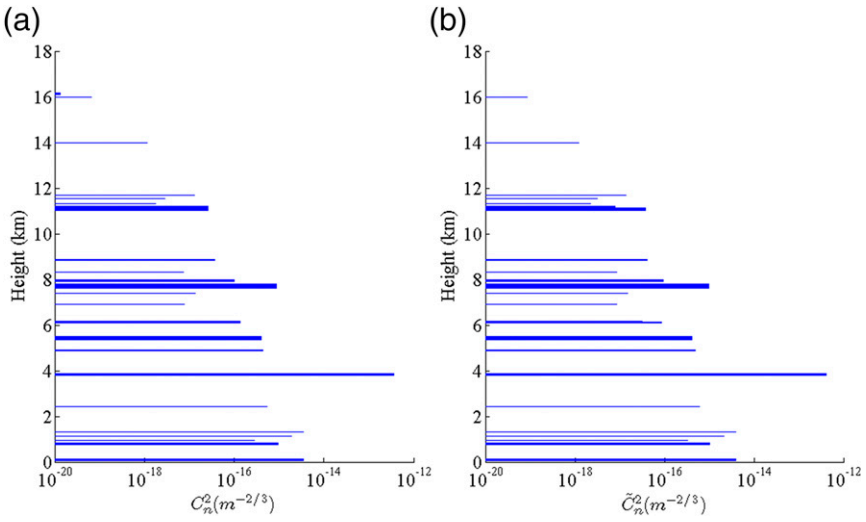

FIG. 13. Turbulence intensity profiles derived from a single radiosonde launch at Miami at 1200 UTC 15 Jan 2008. (a) Result obtained from actual radiosonde data. (b) Result obtained after injecting the radiosonde data with the following errors: $\varepsilon_T = 0.3$ K, $\varepsilon_p = 5\%$, and $e_{\mathrm{RH}} = 5\%$.

Sample results of this parametric analysis, representative of the general behavior, are reported in Tables 1 and 2. As can be seen, an error of 0.3 K in absolute temperature, combined with an error of 5% in pressure, provides usually an error smaller than 5% in the C_n^2 profile. On the other hand, an error of 5% in relative humidity implies an error of around 10% in C_n^2. The maximum error in C_n^2, obtained when the largest errors are applied simultaneously to the three atmospheric variables, is usually on the order of 15%. The contribution of the 5% error in pressure to the final error in C_n^2 is typically less than 1% in all the cases.

It is noted that, in general, the introduction of errors into the radiosonde data does not significantly affect the layer distribution, but it alters the corresponding levels of structure constant profiles. The variation is in any case limited, especially in consideration of the degree of uncertainty generally involved in the characterization of turbulence. For the sake of illustration, Fig. 13 reports a comparison between the C_n^2 profiles obtained with and without errors. This example is relevant to the case with the largest errors in the atmospheric variables ($\varepsilon_T = 0.3$ K, $\varepsilon_p = 5\%$, and $\varepsilon_{\mathrm{RH}} = 5\%$), corresponding to a percent error $\varepsilon = 14.6\%$ in C_n^2 according to Eq. (29). As can be seen, the two profiles are qualitatively very similar.

8. Conclusions

A general and self-contained procedure has been presented for deriving from meteorological data the profiles of the refractive index structure constant. Such a procedure is based on the computation of the vertical gradient of the refractive index, and it applies in the troposphere and in the lower stratosphere. This paper differs from previously published approaches in that the objective here is not to derive average C_n^2 profiles based on statistical considerations or a priori assumptions of the vertical outer scale length value, but rather to derive the C_n^2 profile compatible with a given atmospheric scenario. To this end, the local value of the outer scale is calculated from the analysis of the potential temperature profiles by resorting to the Thorpe length concept, and an analysis of the local value of the Richardson's number is used to identify turbulent layers. The procedure has been applied to profiles of the atmospheric variables provided by high-resolution radiosonde data, and the results obtained are in agreement with other results published in the literature. Simulated data provided by LES or NWP models can also be used, provided they have a sufficiently high vertical resolution. The sensitivity of the derived C_n^2 profiles to errors in the atmospheric data has also been investigated, showing good robustness.

The developed procedure can be used to estimate the impact of scintillation disturbances in any microwave link crossing the troposphere, and it is particularly suited to evaluate through simulations the performances of atmosphere sounding techniques in the presence of turbulence. The integration of the derived C_n^2 profiles into a simulation tool for the prediction of scintillation effects will be the subject of a future work, devoted to analyzing the performance of NDSA for water vapor retrieval in the 19–32-GHz interval and above 170 GHz.

Acknowledgments. This study has been supported by the European Space Agency through Contract 4000104831 [Analysis of Normalised Differential Spectral Attenuation (NDSA) Technique for Inter-Satellite Atmospheric Profiling].

REFERENCES

Andreas, E. L, 1988: Estimating C_n^2 over snow and sea ice from meteorological data. *J. Opt. Soc. Amer.*, **5A**, 481–495, doi:10.1364/JOSAA.5.000481.

Arneodo, A., and Coauthors, 1996: Structure functions in turbulence, in various flow configurations, at Reynolds number between 30 and 5000, using extended self-similarity. *Europhys. Lett.*, **34**, 411, doi:10.1209/epl/i1996-00472-2.

Barat, J., and F. Bertin, 1984: Simultaneous measurements of temperature and velocity fluctuations within clear air turbulence layers: Analysis of the estimate of dissipation rate by remote sensing techniques. *J. Atmos. Sci.*, **41**, 1613–1619, doi:10.1175/1520-0469(1984)041<1613:SMOTAV>2.0.CO;2.

Brettle, M. J., and J. F. P. Galvin, 2003: Back to basics: Radiosondes: Part 1—The instrument. *Weather*, **58**, 336–341, doi:10.1256/wea.126.02A.

Burk, S. D., 1980: Refractive index structure parameters: Time-dependent calculations using a numerical boundary-layer model. *J. Appl. Meteor.*, **19**, 562–576, doi:10.1175/1520-0450(1980)019<0562:RISPTD>2.0.CO;2.

Cheinet, S., and A. P. Siebesma, 2009: Variability of local structure parameters in the convective boundary layer. *J. Atmos. Sci.*, **66**, 1002–1017, doi:10.1175/2008JAS2790.1.

Cherubini, T., S. Businger, R. Lyman, and M. Chun, 2008: Modeling optical turbulence and seeing over Mauna Kea. *J. Appl. Meteor. Climatol.*, **47**, 1140–1155, doi:10.1175/2007JAMC1487.1.

Clayson, C. A., and L. Kantha, 2008: On turbulence and mixing in the free atmosphere inferred from high-resolution soundings. *J. Atmos. Oceanic Technol.*, **25**, 833–852, doi:10.1175/2007JTECHA992.1.

Coulman, C. E., J. Vernin, Y. Coqueugniot, and J.-L. Caccia, 1988: Outer scale of turbulence appropriate to modeling refractive-index structure profiles. *Appl. Opt.*, **27**, 155, doi:10.1364/AO.27.000155.

Crain, C. M., 1950: Apparatus for recording fluctuations in the refractive index of the atmosphere at 3.2 centimeters wavelength. *Rev. Sci. Instrum.*, **21**, 456–457, doi:10.1063/1.1745614.

——, 1955: Survey of airborne microwave refractometer measurements. *Proc. IRE*, **43**, 1405–1411, doi:10.1109/JRPROC.1955.277956.

D'Auria, G., F. S. Marzano, and U. Merlo, 1993: Model for estimating the refractive-index structure constant in clear-air intermittent turbulence. *Appl. Opt.*, **32**, 2674–2680, doi:10.1364/AO.32.002674.

Deardorff, J. W., 1974: Three-dimensional numerical study of turbulence in an entraining mixed layer. *Bound.-Layer Meteor.*, **7**, 199–226, doi:10.1007/BF00227913.

Ebisuzaki, W., 2004: Data documentation for NOAA Operational Model Archive and Distribution System (NOMADS): North American Regional Reanalysis (NARR) "merge" data set; Dataset DSI-6175, NOAA, 11 pp. [Available online at http://nomads.ncdc.noaa.gov/docs/ncdc-narrdsi-6175-final.pdf.]

Facheris, L., F. Cuccoli, and F. Argenti, 2008: Normalized differential spectral attenuation (NDSA) measurements between two LEO satellites: Performance and analysis in the Ku/K-bands. *IEEE Trans. Geosci. Remote Sens.*, **46**, 2345–2356, doi:10.1109/TGRS.2008.917215.

Galvin, J. F. P., 2003: Back to basics: Radiosondes: Part 2—Using and interpreting the data. *Weather*, **58**, 387–395, doi:10.1256/wea.126.02B.

Ghosh, A. K., A. R. Jain, and V. Sivakumar, 2003: Simultaneous MST radar and radiosonde measurements at Gadanki (13.5°N, 79.2°E) 2. Determination of various atmospheric turbulence parameters. *Radio Sci.*, **38**, 1014, doi:10.1029/2000RS002528.

Gossard, E. E., R. B. Chadwick, W. D. Neff, and K. P. Moran, 1982: The use of ground-based Doppler radars to measure gradients, fluxes and structure parameters in elevated layers. *J. Appl. Meteor.*, **21**, 211–226, doi:10.1175/1520-0450(1982)021<0211:TUOGBD>2.0.CO;2.

Hill, R. J., R. A. Bohlander, S. F. Clifford, R. W. McMillan, J. T. Priestly, and W. P. Schoenfeld, 1988: Turbulence-induced millimeter-wave scintillation compared with micrometeorological measurements. *IEEE Trans. Geosci. Remote Sens.*, **26**, 330–342, doi:10.1109/36.3035.

Holdrige, D., J. Prell, M. Ritsche and R. Coulter, 2011: Balloon-Borne Sounding System (SONDE) handbook. ARM Tech. Rep. DOE/SC-ARM/TR-029, 27 pp.

Hufnagel, R. E., 1978: Propagation through atmospheric turbulence. *The Infrared Handbook*, W. L. Wolfe and G. J. Zissis, Eds., Office of Naval Research, 1–56.

Ishimaru, A., 1999: *Wave Propagation and Scattering in Random Media*. John Wiley & Sons, 600 pp.

Karasawa, Y., M. Yamada, and J. E. Allnut, 1988: A new prediction method for tropospheric scintillation on Earth-space paths. *IEEE Trans. Antennas Propag.*, **36**, 1608–1614, doi:10.1109/8.9712.

Kolmogorov, N., 1962: A refinement of previous hypotheses concerning the local structure of turbulence in a viscous incompressible fluid at high Reynolds number. *J. Fluid Mech.*, **13**, 82–85, doi:10.1017/S0022112062000518.

Lüdi, A., and A. Magun, 2002: Near-horizontal line-of-sight millimeter-wave propagation measurements for the determination of outer length scales and anisotropy of turbulent refractive index fluctuations in the lower troposphere. *Radio Sci.*, **37**, 1028, doi:10.1029/2001RS002493.

Luers, J. K., 1997: Temperature error of the Vaisala RS90 radiosonde. *J. Atmos. Oceanic Technol.*, **14**, 1520–1532, doi:10.1175/1520-0426(1997)014<1520:TEOTVR>2.0.CO;2.

Martini, E., A. Freni, F. Cuccoli, and L. Facheris, 2006: The impact of tropospheric scintillation in the Ku/K bands on the communications between two LEO satellites in a radio occultation geometry. *IEEE Trans. Geosci. Remote Sens.*, **44**, 2063–2071, doi:10.1109/TGRS.2006.872143.

Masciadri, E., J. Vernin, and P. Bougeault, 1999a: 3D mapping of optical turbulence using an atmospheric numerical model. I. A useful tool for the ground-based astronomy. *Astron. Astrophys. Suppl. Ser.*, **137** 185–202, doi:10.1051/aas:1999474.

——, ——, and ——, 1999b: 3D mapping of optical turbulence using an atmospheric numerical model. II. First results at Cerro Paranal. *Astron. Astrophys. Suppl. Ser.*, **137**, 203–216, doi:10.1051/aas:1999475.

Mason, P. J., 1989: Large-eddy simulation of the convective atmospheric boundary layer. *J. Atmos. Sci.*, **46**, 1492–1516, doi:10.1175/1520-0469(1989)046<1492:LESOTC>2.0.CO;2.

Moeng, C.-H., 1984: A large-eddy-simulation model for the study of planetary boundary-layer turbulence. *J. Atmos. Sci.*, **41**, 2052–2062, doi:10.1175/1520-0469(1984)041<2052:ALESMF>2.0.CO;2.

Monin, A. S., and A. M. Obukhov, 1954: Basic laws of turbulent mixing in the surface layer of the atmosphere. *Tr. Geofiz. Inst., Akad. Nauk SSSR*, **24**, 163–187.

Nath, D., M. Venkat Ratnam, A. K. Patra, B. V. Krishna Murthy, and S. V. Bhaskar Rao, 2010: Turbulence characteristics over tropical station Gadanki (13.5°N, 79.2°E) estimated using high-resolution GPS radiosonde data. *J. Geophys. Res.*, **115**, D07102, doi:10.1029/2009JD012347.

Nightingale, N. S., and D. F. Buscher, 1991: Interferometric seeing measurements at the La Palma Observatory. *Mon. Not. Roy. Astron. Soc.*, **251**, 155–166, doi:10.1093/mnras/251.1.155.

Ottersten, H., 1969: Mean vertical gradient of potential refractive index in turbulent mixing and radar detection of CAT. *Radio Sci.*, **4**, 1247–1249, doi:10.1029/RS004i012p01247.

Otung, I. E., 1996: Prediction of tropospheric amplitude scintillation on a satellite link. *IEEE Trans. Antennas Propag.*, **44**, 1600–1608, doi:10.1109/8.546246.

Peltier, L. J., and J. C. Wyngaard, 1995: Structure-function parameters in the convective boundary layer from large-eddy simulation. *J. Atmos. Sci.*, **52**, 3641–3660, doi:10.1175/1520-0469(1995)052<3641:SPITCB>2.0.CO;2.

Pereira, C., C. Ghiringhelli, and D. Vanhoenacker-Janvier, 2015: Sensitivity of tropospheric scintillation models to the accuracy of radiosonde data. *2015 9th European Conference on Antennas and Propagation (EuCAP)*, IEEE, 3205–3208.

Rees, J. M., 1991: On the characteristics of eddies in the stable atmospheric boundary layer. *Bound.-Layer Meteor.*, **55**, 325–343, doi:10.1007/BF00119808.

Rosenberg, N. W., and E. M. Dewan, 1975: Stratospheric turbulence and vertical effective diffusion coefficients. Air Force Cambridge Research Laboratories Tech. Rep. AFCRL-TR-75-0519, 13 pp.

Siebesma, A. P., and A. M. Holtslag, 1996: Model impacts of entrainment and detrainment rates in shallow cumulus convection. *J. Atmos. Sci.*, **53**, 2354–2364, doi:10.1175/1520-0469(1996)053<2354:MIOEAD>2.0.CO;2.

Smith, E. K., and S. Weindtraub, 1953: The constants in the equation for atmospheric refractive index at radio frequencies. *Proc. IRE*, **41**, 1035–1037, doi:10.1109/JRPROC.1953.274297.

Stephens, G. L., 1984: The parameterization of radiation for numerical weather prediction and climate models. *Mon. Wea. Rev.*, **112**, 826–867, doi:10.1175/1520-0493(1984)112<0826:TPORFN>2.0.CO;2.

Tatarskii, V. I., 1961: *Wave Propagation in a Turbulent Medium*. McGraw-Hill, 285 pp.

Taylor, G. I., 1931: Effect of variation in density on the stability of superposed streams of fluid. *Proc. Roy. Soc. London*, **132A**, 499–523, doi:10.1098/rspa.1931.0115.

Thorpe, S. A., 1977: Turbulence and mixing in a Scottish Loch. *Philos. Trans. Roy. Soc. London*, **286A**, 125–181, doi:10.1098/rsta.1977.0112.

Turner, J. S., 1973: *Buoyancy Effects in Fluid*. Cambridge University Press, 368 pp.

Vanhoenacker-Janvier, D., C. Oestges, B. Montenegro-Villacieros, R. Van Malderen, and H. De Backer, 2009: Scintillation prediction using improved pre-processed radiosounding data. *2009 3rd European Conference on Antennas and Propagation*, IEEE, 3849–3851.

Van Zandt, T. E., J. L. Green, K. S. Gage, and W. L. Clark, 1978: Vertical profiles of refractivity turbulence structure constant: Comparison of observations by the Sunset Radar with a new theoretical model. *Radio Sci.*, **13**, 819–829, doi:10.1029/RS013i005p00819.

——, K. S. Gage, and J. Warnock, 1981: An improved model for the calculation of profiles of C_n^2 and n in the free atmosphere from background profiles of wind, temperature and humidity. Preprints, *20th Conf. on Radar Meteorology*, Boston, MA, Amer. Meteor. Soc., 129–135.

Vasseur, H., 1999: Prediction of tropospheric scintillation on satellite links from radiosonde data. *IEEE Trans. Antennas Propag.*, **47**, 293–301, doi:10.1109/8.761069.

——, and D. Vanhoenacker, 1998: Characterisation of tropospheric turbulent layers from radiosonde data. *Electron. Lett.*, **34**, 318–319, doi:10.1049/el:19980248.

Wesely, M. L., 1976: The combined effect of temperature and humidity fluctuations on refractive index. *J. Appl. Meteor.*, **15**, 43–49, doi:10.1175/1520-0450(1976)015<0043:TCEOTA>2.0.CO;2.

Wheelon, A. D., 2001: *Geometrical Optics*. Vol.1, *Electromagnetic Scintillation*, Cambridge University Press, 455 pp.

——, 2003: *Weak Scattering*. Vol. 2, *Electromagnetic Scintillation*, Cambridge University Press, 440 pp.

Wyngaard, J. C., W. T. Pennell, D. H. Lenschow, and M. A. Lemone, 1978: The temperature-humidity covariance budget in the convective boundary layer. *J. Atmos. Sci.*, **35**, 47–58, doi:10.1175/1520-0469(1978)035<0047:TTHCBI>2.0.CO;2.

Ziad, A., M. Schock, G. A. Chanan, M. Troy, R. Dekany, B. F. Lane, J. Borgnino, and F. Martin, 2004: Comparison of measurements of the outer scale of turbulence by three different techniques. *Appl. Opt.*, **43**, 2316–2324, doi:10.1364/AO.43.002316.